



# Tunneling Processes Induced by Terahertz Electric Fields

S.D. GANICHEV<sup>1,2</sup>, I.N. YASSIEVICH<sup>2</sup> and W. PRETTL<sup>1</sup>

<sup>1</sup>*Institut für Experimentelle und Angewandte Physik, Universität Regensburg 93040 Regensburg, Germany*

<sup>2</sup>*A.F. Ioffe Physico-Technical Institute, Russian Academy of Sci. 194021 St. Petersburg, Russia*

**Abstract.** Tunneling processes induced by terahertz frequency electric fields have been investigated. A drastic enhancement of the tunneling probability has been observed by increasing the frequency  $\omega$  at  $\omega\tau_e \gg 1$  where  $\tau_e$  is the tunneling time. For a given constant tunneling rate an increase of frequency by a factor of seven leads to a drop of the required electric field strength by three orders of magnitude. It is shown that the enhancement of tunneling ionization at terahertz frequencies is due to the fact that electrons can absorb energy from the radiation field during tunneling reducing the effective width of the tunneling barrier.

**Key words:** Electron and nucleus tunneling, terahertz fields

## 1. Introduction

Tunneling as a manifestation of quantum mechanics is of great importance for many systems in physics, chemistry and biology. In the last decade electron transfer by tunneling, which play a key role in living systems, has attracted considerable attention (see e.g. [1, 2]). The long-range transfer of electrons occurs in many biological systems and is a process with inherently quantum mechanical aspects. The dynamics of such reactions depends on both tunneling of the electrons and the nuclear rearrangements of the protein itself [3]. Here we report on tunneling induced by high-intensity terahertz (THz) radiation. Using the electric field of short laser pulses at THz frequencies permits contactless and uniform application of high electric field strengths. Our measurements have been carried out on deep impurities in semiconductors which represent a model for nuclear tunneling between adiabatic potentials and electron tunneling through the potential well formed by the electron attracting force of the impurity and the alternating electric field of the high frequency radiation. We expect that the THz-tunneling method reported here on impurities in semiconductors, in particular the recently observed enhancement of tunneling by contactless application of coherent radiation [4], may also be applied to biological molecules in order to investigate tunneling reactions and pathways.

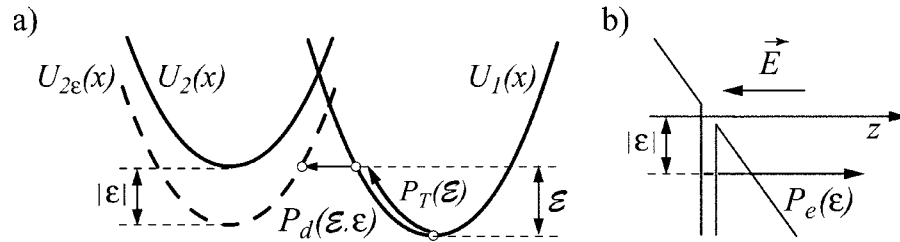


Figure 1. Illustration of the tunneling ionization of deep centers in a static electric field: a) thermal excitation and defect tunneling, b) electron tunneling with probabilities  $P_T(\varepsilon)$ ,  $P_d(\varepsilon, \varepsilon)$  and  $P_e(\varepsilon)$ , respectively. The energy of both the vibrating defect and the electron is shown as a function of a configuration coordinate  $x$  for the electron bound to ( $U_2$ ) and detached from ( $U_1$ ) the defect. The potential plotted in broken lines corresponds to an electron with negative kinetic energy which has been detached from the impurity by tunneling in the external electric fields shown in (b). Arrows indicate tunneling trajectories.

To apply high frequency electric fields the terahertz radiation field of a pulsed far-infrared gas laser optically pumped by TEA-CO<sub>2</sub> laser has been used yielding 40 ns pulses with intensity up to 5 MW/cm<sup>2</sup> between one and 5 THz [5]. It is shown that impurity ionization occurs by phonon assisted tunneling [6, 7] which proceeds at high electric field strengths into direct tunneling without involving phonons. In the quasi-static regime of relatively low frequencies the tunneling probability is independent on frequency. The dependence of the ionization probability on the electric field strength permits to determine defect tunneling times [7–9], the structure of the adiabatic potentials of the defect and the strength of electron-phonon interaction. Raising the frequency leads to a drastical enhancement of tunneling ionization [4, 10]. For a given constant tunneling rate an increase of frequency by a factor of seven leads to a drop of the required electric field strength by three orders of magnitude. The transition from the quasi-static limit to frequency dependent tunneling, for the first time worked out theoretically by L.V. Keldysh [11], is determined by the tunneling time. The enhancement of tunneling occurs when the frequency gets larger than the inverse tunneling time. This limit is approached in the terahertz regime.

## 2. Theoretical Consideration

The tunneling ionization will be treated in semi-classical approximation in the adiabatic limit. In most cases deep impurities have one bound state which phenomenologically can be approximated by a potential well. Due to electron-phonon interaction the system consisting of local impurity vibrations and an electron is characterized by two adiabatic potentials  $U_1(x)$  and  $U_2(x)$  as a function of a configuration coordinate  $x$  [12]. These adiabatic potentials correspond to the electron bound to the impurity and the electron detached from the impurity with zero kinetic energy, respectively (see Figure 1). The energy separation between minima of

$U_1(x)$  and  $U_2(x)$  is the thermal ionization energy of the electron  $\varepsilon_T$ . In the case when a free electron has the kinetic energy  $\varepsilon$ , the adiabatic potential is  $U_{2\varepsilon}(x) = U_2(x) + \varepsilon$ .

The ionization of deep impurities in an electric field is achieved by two simultaneous tunneling processes, the tunneling of the defect nucleus, with probability  $P_d$  (see Figure 1a) and electron tunneling through the triangular potential barrier formed by the impurity potential well and the electric field (see inset in Figure 1b) with probability  $P_e$ . The defect ionization is accomplished by thermal excitation of the system in the adiabatic bound state potential  $U_1(x)$  to a vibrational energy  $\mathcal{E}$  and tunneling of the impurity configuration from this state into the ionized configuration  $U_2(x)$  [7]. The application of an electric field  $E = E_0 \cos(\omega t)$  leads to electron tunneling. Thus, electrons can be emitted at a negative kinetic energy  $\varepsilon < 0$  which shifts the adiabatic potential of the ionized configuration  $U_2(x)$  to a lower energy and, hence, increases the ionization probability.

The ionization probability is given by:

$$e(E) = \iint P_e P_d \exp(-\mathcal{E}/k_B T) d\varepsilon d\mathcal{E}. \quad (1)$$

The probability of the defect tunneling in the semi-classical approximation is [7, 13]:

$$P_d \propto \exp(-2(S_2 \mp S_1)) \quad (2)$$

where  $S_{1,2}$  is the principal function of defect tunneling under the potential  $U_{1,2}(x)$  multiplied by  $i/\hbar$  [13].

The probability of electron tunneling is [4, 11]:

$$P_e \propto \exp(-2S_e(\varepsilon)) \quad (3)$$

with

$$S_e(\varepsilon) = -\frac{\varepsilon}{\hbar} \int_0^{\tau_e} \frac{1}{\gamma^2} \sinh^2(\omega\tau) d\tau + \frac{\varepsilon\tau_e}{\hbar}. \quad (4)$$

Here  $\gamma \equiv \sqrt{2m^*\varepsilon} \omega/eE$  and  $\tau_e = \hbar \partial S_e / \partial \varepsilon$  has the meaning of an electron tunneling time [9].

At high temperatures and not very high electric field strengths, so that magnitude of the electron energy  $|\varepsilon|$  is smaller than the defect vibration energy  $\mathcal{E}$ , the ionization is caused by phonon assisted tunneling. The electron tunneling time  $\tau_e$  is equal to  $\tau_2 = \hbar \partial |S_2| / \partial \mathcal{E} |_{\varepsilon=0}$ , the time of defect tunneling under the potential  $U_2(x)$ , and the field dependence of the ionization probability is given by [4],

$$e(E) \propto \exp \left[ \frac{E^2}{(E_c^*)^2} \right] \quad \text{with} \quad (E_c^*)^2 = \frac{3m^*\hbar}{e^2(\tau_2^*)^3} \quad (5)$$

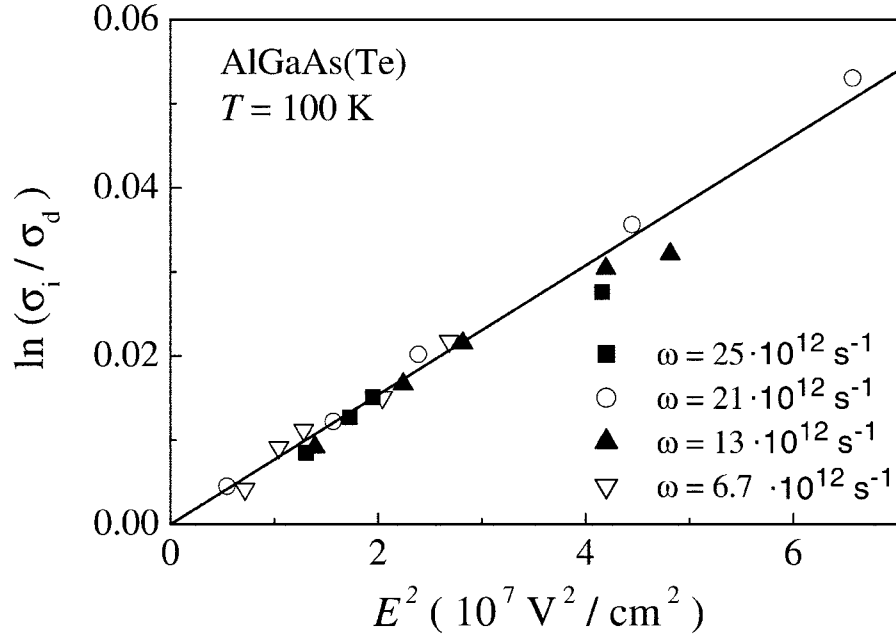


Figure 2. Logarithm of the ratio of the irradiated conductivity,  $\sigma_i$ , to the dark conductivity,  $\sigma_d$ , as a function of the squared electric field,  $E^2$  for  $\text{Al}_{0.35}\text{Ga}_{0.65}\text{As}:\text{Te}$  at  $T = 100$  K for various frequencies  $\omega$ .

$$\text{where } (\tau_2^*)^3 = \frac{3}{4\omega^3}(\sinh(2\omega\tau_2) - 2\omega\tau_2). \quad (6)$$

$$\text{and } \tau_2 = \hbar/2kT \pm \tau_1. \quad (7)$$

Here  $\tau_1 = \hbar\partial|S_1|/\partial\mathcal{E}|_{\varepsilon=0}$  is the time of defect tunneling under the potential  $U_1$  and the plus and minus signs correspond to adiabatic potential configurations of autolocalized and substitutional impurities, respectively [8].

With increasing electric field strength or lowering temperature, so that  $\varepsilon \gg \mathcal{E}$ , the direct carrier tunneling from the ground state into the continuum becomes dominant [7]. This leads to a weaker field dependence of the ionization probability and decreases the tunnelling time with rising electric field strength. Thus at high field strengths  $\omega\tau_2$  becomes smaller than one and the frequency dependence of tunneling vanishes.

### 3. Experimental Results and Analysis

The measurements have been carried out on DX-centers in  $\text{Al}_{0.5}\text{Ga}_{0.5}\text{As}:\text{Te}$  and on Au, Hg and Cu doped Ge in the temperature range in which at thermal equilibrium practically all carriers are bound ( $T = 4.2 - 150$  K). Terahertz electric fields have been applied using a high power line-tunable optically pumped  $\text{NH}_3$  FIR-laser [5]. Electric field strengths up to about 40 kV/cm ( $\simeq 5 \text{ MW}/\text{cm}^2$ ) could be

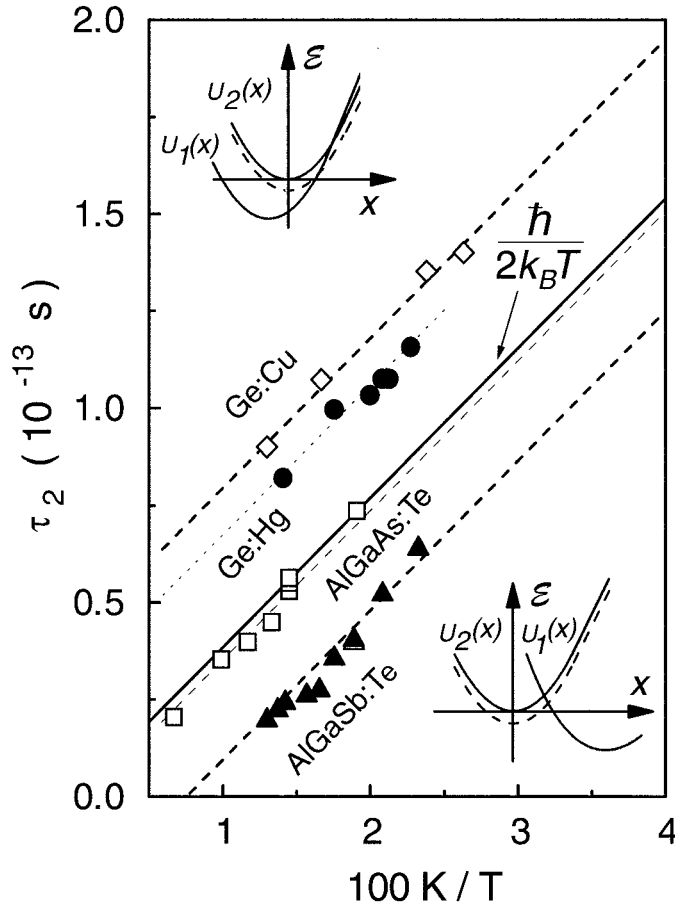


Figure 3. Tunneling time  $\tau_2$  derived from experimental values of  $E_c^2$  versus reciprocal temperature for substitutional impurities (Ge:Cu and Ge:Hg) and DX-centers (AlGaAs:Te and AlGaSb:Te). The full line represents  $\hbar/2k_B T$  and the dashed lines are fits to  $\tau_2 = \hbar/2k_B T \pm \tau_1$ . The line  $\hbar/2k_B T$  separates the range of weak electron-phonon interaction ( $\tau_2 = \hbar/2k_B T + \tau_1$ ) and strong electron-phonon interaction ( $\tau_2 = \hbar/2k_B T - \tau_1$ ). The corresponding adiabatic potentials are shown in the insets top-left and bottom-right. The tunneling time  $\tau_1$  is of the order of  $10^{-14}$  s.

achieved in the frequency range from  $3 \cdot 10^{12} \text{s}^{-1}$  to  $50 \cdot 10^{12} \text{s}^{-1}$  with 40 ns pulses. Irradiation of the samples with terahertz radiation leads to ionization of impurities which is detected by photoconductivity. The ratio of irradiated conductivity and dark conductivity is  $\sigma_i/\sigma_d \propto e(E)/e(0)$  [7].

At sufficiently high temperatures (e.g.  $T = 50 - 100$  K) and in the investigated frequency range, the ionization probability of all materials is observed to be independent on the radiation frequency and increases with rising  $E$  like  $\exp(E^2/E_c^{*2})$  (Figure 2). Thus, the ionization is due to phonon assisted tunneling in the quasi-

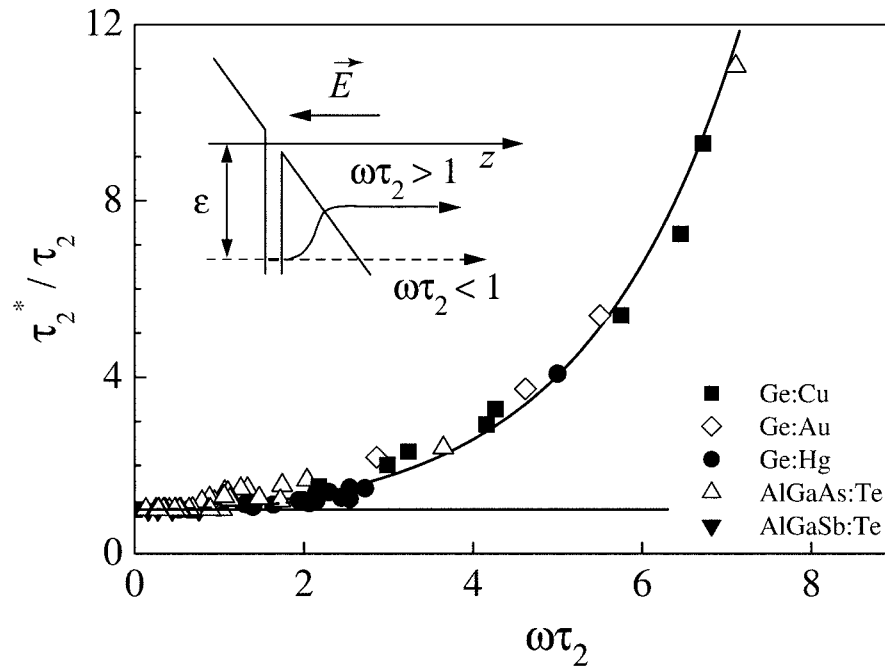


Figure 4. Ratio  $\tau_2^*/\tau_2$  as a function of  $\omega\tau_2$ . The curves show the dependences calculated according to Eq. (6). Experimental results are plotted for all materials, all temperatures, and all radiation frequencies of the present investigation. The inset shows the electron tunneling trajectory in the quasi-static limit (broken line) and the high frequency regime (full line).

static regime (Eq. (5), (6) with  $\omega\tau_2 \ll 1$ ). The electron tunnels at the momentary magnitude of the electric field in a time shorter than the period of oscillation and the electric field acts like a static field (see Figure 1b) [6–8]. As follows from Eqs. (5) the slope of the experimental curves in the field region where  $\ln(\sigma_i/\sigma_d) \propto \exp(E^2/E_c^2)$  permits the determination of the tunneling time  $\tau_2$ . In Figure 3 the tunneling time  $\tau_2$  is shown as a function of the reciprocal temperature. For comparison, Figure 3 shows also a plot of  $\hbar/2k_B T$ . We see that  $\tau_2$  is of the order of  $\hbar/2k_B T$ . Note, however, an essential point. As evident from the experimental data presented in Figure 3,  $\tau_2$  is larger than  $\hbar/2k_B T$  for substitutional impurities, but less than  $\hbar/2k_B T$  for auto-localized DX-centers. This result is in excellent agreement with theory (see Eq. (7)). The frequency independent tunneling is limited to  $\omega\tau_2 \leq 1$ .

Lowering the temperature leads to an increase of  $\tau_2$  (see Eq. (7)) and thus  $\omega\tau_2$  becomes larger than one. In this case the ionization probability is observed to be still depended exponentially on  $E^2$ , but the magnitude of  $E_c^*$  decreases strongly with increasing frequency. Varying the temperature and the radiation frequency the dependence of the effective time  $\tau_2^*$  has been obtained from measured values of  $E_c^*$ . In Figure 4 the ratio  $\tau_2^*/\tau_2$  determined experimentally is plotted as a function of  $\omega\tau_2$  and compared to calculations after Eq. (6). In contrast to static electric fields

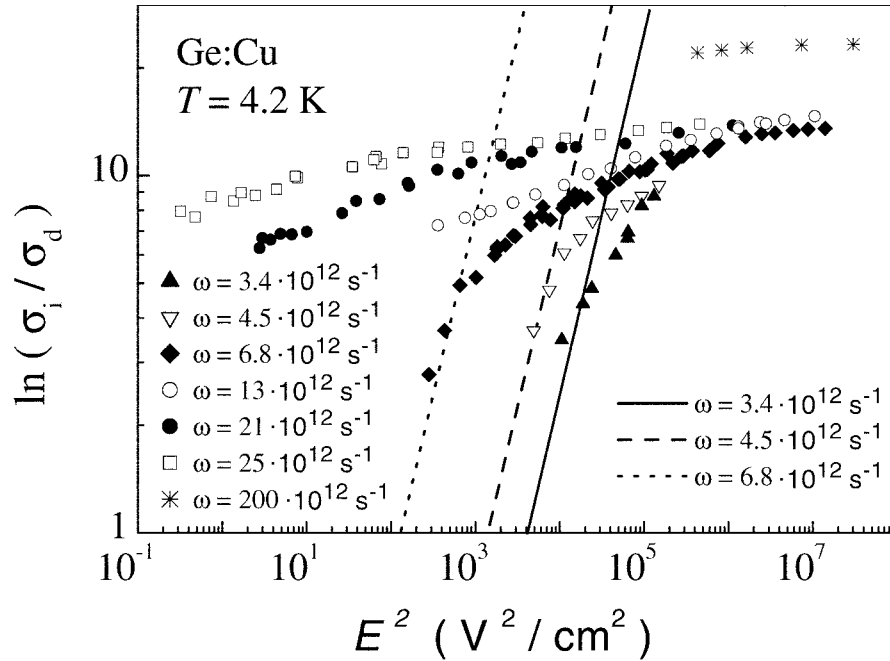


Figure 5.  $\ln(\sigma_i/\sigma_d)$  for Ge:Cu as a function of  $E^2$  for different frequencies  $\omega$  at liquid helium temperature. Lines show calculations after Eq. (1)-(4) for the three lowest frequencies used in experiment.

where the electron tunnels at a fixed energy, in alternating fields the energy of the electron is not conserved during tunneling (see inset in Figure 4). In this case the electron can absorb energy from the field, which leads to a sharp increase of the tunneling probability with rising frequency.

Further decrease of the temperature leads to a much stronger frequency dependence of the ionization probability due to the fact that at e.g. 4.2 K and at low field strengths the condition  $\omega\tau_2 \gg 1$  is valid for the whole frequency range investigated here. Such a drastic frequency dependence, which is observed for all samples, is shown in Figure 5 for Ge:Cu at 4.2 K. It is seen that at relatively low field strength for a given constant signal a change of six orders of magnitude of  $E^2$  needs only a seven times change in frequency  $\omega$ . In order to display in one figure the total set of data covering eight orders of magnitude in the square of the electric field,  $\log(E^2)$  has been plotted on the abscissa. To make an easy comparison to the  $\exp(E^2/E_c^2)$  dependence of  $\sigma_i/\sigma_d$  possible, a  $\log \log$  presentation has been used for the ordinate. For the three lowest frequencies  $\omega = 3.4 \cdot 10^{12} \text{s}^{-1}$ ,  $\omega = 4.5 \cdot 10^{12} \text{s}^{-1}$  and  $\omega = 6.8 \cdot 10^{12} \text{s}^{-1}$  and not to high electric field strengths, the ionization probability can be described in terms of phonon assisted tunneling  $e(E) \propto \exp(E^2/E_c^{*2})$  as it was the case for all frequencies at higher temperatures (the lines in Figure 5).

However, at higher field strength, the field dependence of the emission probability is much weaker and the frequency dependence practically disappears. This

effect is the result of the transition from phonon assisted tunneling to direct tunneling without involving phonons which is characterized by a weaker growth of the ionization probability in comparison to the field dependence of phonon assisted tunneling [7]. The calculations after Eq. (1-4) for Ge:Cu at 4.2 K and for the frequencies used in the experiments taking into account both processes, phonon assisted tunneling and direct tunneling, show that the theory describes qualitatively well all experimentally observed features of the field and frequency dependence of tunneling ionization. The disappearance of the frequency effect at very high fields can be explained by the electric field dependence of the tunneling time  $\tau_2$ . In the high field regime the defect tunneling trajectory is shifted to lower energies leading to a decrease of  $\tau_2$ . By this  $\omega\tau_2$  becomes smaller than one and the frequency dependence vanishes.

### Acknowledgements

Financial support by the DFG and the RFFI are gratefully acknowledged.

### References

1. Kuki, A. and Wolynes, P.G.: Electron Tunneling Paths in Proteins, *Science* **236** (1987), 1647–1652.
2. Balabin, I.A. and Onuchic, J.N.: Dynamically Controlled Protein Tunneling Paths in Photosynthetic Reaction Centers, *Science* **290** (2000), 114–117.
3. Chance, B., Devault, D.C., Frauenfelder, H., Marcus, R.A., Schrieffer, J.R. and Sutin, N. (eds.): *Tunneling in Biological Systems*, Academic Press, New York, 1979, pp. 1–758.
4. Ganichev, S.D., Ziemann, E., Gleim, Th., Prettl, W., Yassievich, I.N., Perel, V.I., Wilke, I. and Haller, E.E.: Carrier Tunneling in High-Frequency Electric Fields, *Phys. Rev. Lett.* **80** (1998), 2409–2412.
5. Ganichev, S.D.: Tunnel Ionization of Deep Impurities in Semiconductors induced by Terahertz Electric Fields, *Physica B* **273-274** (1999), 737–742.
6. Ganichev, S.D., Prettl, W. and Huggard, P.G.: Phonon assisted Tunnel Ionization of Deep Impurities in the Electric Field of Far-Infrared Radiation, *Phys. Rev. Lett.* **71** (1993), 3882–3885.
7. Ganichev, S.D., Prettl, W. and Yassievich, I.N.: Ionization of Deep Impurities by Far-Infrared Radiation, *Phys. Solid State* **39** (1997), 1703–1726.
8. Ganichev, S.D., Diener, J., Yassievich, I.N., Prettl, W., Meyer, B.K. and Benz, K.W.: Tunnelling Ionization of Autolocalized DX-centers in Terahertz Fields, *Phys. Rev. Lett.* **75** (1995), 1590–1593.
9. Büttiker, M. and Landauer, R.: Traversal Time of Tunneling, *Phys. Rev. Lett.* **49** (1982), 1739–1742.
10. Ganichev, S.D., Ketterl, H., Perel, V.I., Yassievich, I.N. and Prettl, W.: Tunneling Ionization of Deep Centers in High-Frequency Electric Fields, *Phys. Rev. B.* **65** (2002), 085203-1-9.
11. Keldysh, L.V.: Ionization of Atoms in a Strong Electric Fields, *Sov. Phys. JETP* **20** (1965), 1307–1310.
12. Abakumov, V.N., Perel, V.I. and Yassievich, I.N.: Nonradiative Recombination in Semiconductors, In: V.M. Agranovich and A.A. Maradudin (eds.), *Modern Problems in Condensed Matter Sciences* Vol. **33**, North Holland, Amsterdam, 1991, pp. 1–320.
13. Landau, L.D. and Livshitz, E.M.: *Quantum Mechanics*, Pergamon Press, Oxford, 1977, p. 287.